

## The Effect of Intermediate Heat Treatment on the Anisotropy of Ferritic ODS Steel

Min Kyeong Seo, Hyoung Kee Min, Suk Hoon Kang\*, Young Bum Chun, Sang Hoon Noh, Tae Kyu Kim  
Nuclear Materials Division, Korea Atomic Energy Research Institute,  
989-111 Daedeok-daero, Yuseong-gu, Daejeon, 305-353, Korea.

\*Corresponding author: shkang77@kaeri.re.kr

### 1. Introduction

The use of oxide dispersion strengthened (ODS) steels improves creep strength and oxidation/corrosion resistance at high temperatures and consequently increases the operating temperature of cladding tubes in nuclear reactors by approximately 700°C or higher [1-3]. However, the manufacturing of ODS cladding tubes is difficult; ODS steel tubes usually reveal an anisotropic strength in the hoop and longitudinal directions owing to a strongly elongated grain morphology [4-6]. Solutions to this problem involve a phase transformation for 9-11%Cr ODS steel and recrystallization heat treatment for 12-20%Cr ODS steel. Those solutions can effectively modify the strength anisotropy of ODS steel. To overcome the anisotropy problem during the cold rolling of ferritic ODS steel, recrystallization for the elongated grains along the rolling direction is applied by intermediate heat treatment. Recrystallized grains are coarser and equiaxial, and they significantly improve the ductility and high-temperature strength in the hoop direction.

This study focused on the effect of intermediate heat treatment whenever the cold rolling reduction ratio reaches approximately 40%, and the corresponding micro hardness and grain shape variations were investigated. In Particular, the evolution and extinction of specific crystallographic textures were observed during cold rolling and intermediate heat treatment to quantify the uniformity of the microstructure.

### 2. Methods and Results

#### 2.1 Methods

The material used in this study was ferritic ODS steel having the chemical composition shown in Table I. A relatively high content of chromium was used to enhance the corrosion resistance, and molybdenum was used instead of a tungsten as a solid solution hardening element in the matrix. 2% of tungsten was effective for enhancing tensile property of ODS steel, however, the activation properties of tungsten are suspected to be inadequate, neutron radiation causes an embrittlement of tungsten.

Table I. Chemical composition (wt.%) of 15Cr ODS steel.

Cr	Mo	Ti	Y <sub>2</sub> O <sub>3</sub>	Fe
15	1	0.3	0.35	Bal.

Fe-15Cr powders were mechanically alloyed (MA) with 0.3wt% Ti and 0.35wt% Y<sub>2</sub>O<sub>3</sub> powders in a high

energy miller (CM 20) at 240rpm for 48hours. The MA powders were placed in an AISI 304L stainless steel container, sealed after a degassing process, and consolidated by a hot isostatic pressing process at 1150°C under a pressure of 100MPa for 3hours. A hot isostatic pressed billet was hot-rolled at 1150°C into a plate with a reduction ratio of 40%. The cold rolling was performed twice with a reduction ratio of 40% in each stage to fabricate a cold rolled sample with a thickness of 0.5mm. The intermediate heat treatment was conducted at 1150°C for 4minutes after the first stage of the cold rolling. A cold-rolled sample was heat-treated at 1150°C for 1hour.

#### 2.2 Results

The workability of steel can be estimated by the hardness measurement during manufacturing. The reduction ratio of the cold rolling process was designed to refer to the adequate hardness level. Figure 1 shows the plot of micro hardness variations during cold rolling processes. All process steps are identified by alphabet characters, (a) after hot rolling, (b) cold rolling, 40% reduction ratio, (c) intermediate heat treatment, 1150°C for 4hour, (d) cold rolling, 80% reduction ratio, (e) intermediate heat treatment, 1150°C for 4hour, and (f) cold rolling 87.5% reduction ratio. Higher levels of hardness are shown in steps (b), (d) and (f), which were designed to be less than 400Hv after that process. After each rolling process, intermediated heat treatments were conducted, the effects of which are shown in steps (c) and (e).

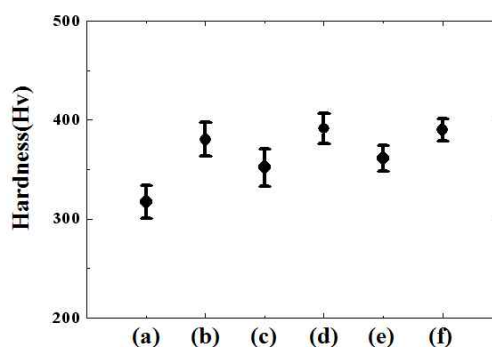


Fig. 1. Cold rolling processes and corresponding micro hardness variations.

It was suspected that recrystallized grains during intermediated heat treatment are coarser and equiaxial. Figure 2 shows the microstructure variations during the cold rolling process of 15Cr ODS steel. In figure 2(a),

bi-modal grain distributions were observed, and the grains were inhomogeneous just after the hot rolling process. In figure 2(b), a deformed microstructure was observed, and the grain sizes were refined. The high fraction of  $\langle 100 \rangle // ND$  and  $\langle 111 \rangle // ND$  textures were shown by the red and blue colors, respectively, and their distribution were related to the evolution of a typical BCC rolling texture. In figure 2(c), a high fraction of recrystallized grains is shown, the grain sizes of which were 3-5 times bigger than the deformed grains in figure 2(b). The  $\langle 100 \rangle // ND$  and  $\langle 111 \rangle // ND$  textures were partially disappeared, and the preferred orientation was slightly moved to  $\langle 112 \rangle // ND$  (purple). In figure 2(d), a recrystallized grains were deformed again, higher fraction of grain boundaries was observed, and the  $\langle 100 \rangle // ND$  and  $\langle 111 \rangle // ND$  textures were developed. In figure 2(e), a similar evolution of recrystallized microstructure as observed in figure 2(d) was shown. In figure 2(f), the microstructure of a 87.5% cold rolled specimen was shown. In figures 2(c) and 2(e), the effects of intermediated heat treatment were qualitatively observed. However, the results can be analyzed quantitatively using an orientation distribution function (ODF) map, as shown in figure 3. The typical BCC rolling textures are consist of conventional  $\alpha$  and  $\gamma$  fiber textures, which are  $\langle 110 \rangle // RD$  and  $\langle 111 \rangle // ND$ , respectively. In particular,  $\langle 110 \rangle // RD$ ,  $\langle 100 \rangle // ND$  texture is called rotated cube texture ' $\langle 110 \rangle \{001\}$ '. The quantification of  $\alpha$  and  $\gamma$  fiber texture can describe the anisotropy of cold rolled BCC material. On the right side of figure 3, the intensity levels of the fiber textures are shown by contours and corresponding numbers (1-7). This suggests that the intensity of the specific texture is 1-7 times bigger than the intensity of isotropic the distribution. In figures 3(b), 3(d), 3(f), the intensity of the  $\alpha$  and  $\gamma$  fiber textures increased to 7, and the anisotropy was enhanced. However, in figure 3(c) and 3(e), the intensity of the  $\alpha$  and  $\gamma$  fiber textures decreased to 3, and the isotropy was enhanced. It was observed that the intermediated heat treatment was effective in enhancing the isotropy of a cold rolled specimen.

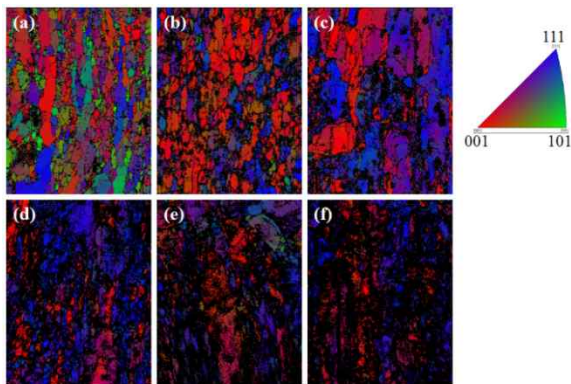


Fig. 2. EBSD images of microstructure variations during the cold rolling process.

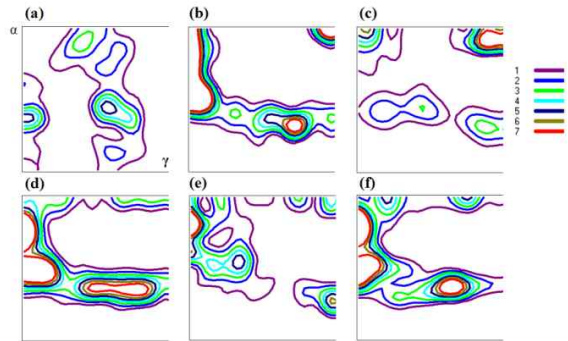


Fig. 3. Orientation distribution function map of 15Cr ODS steel during the cold rolling process.

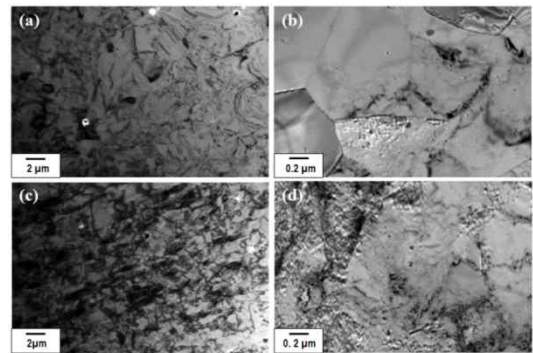


Fig. 4. TEM images of (a),(b) as hot rolled, (c),(d) 87.5% cold rolled.

Figure 4 shows the TEM bright field image of 15Cr ODS steel before and after the cold rolling processes. The average grain size was estimated as  $2\mu m$  just after the hot rolling process; This was refined to  $750nm$  after cold rolling process. Oxide particles are evenly distributed in the matrix and the sizes are  $5-10nm$ . They were stable through the whole manufacture processes of the rolling and intermediate heat treatment.

### 3. Conclusions

The quantification of  $\alpha$  and  $\gamma$  fiber textures can describe the anisotropy, and the intensity of  $\alpha$  and  $\gamma$  fiber textures decreased from 7 to 3 by intermediate heat treatment. Intermediate heat treatment relaxed the internal stress of ODS steel and reduced the anisotropy by the recrystallization of the materials.

### REFERENCES

- [1] A. Alamo, V. Lambard, X. Averty, and M.H. Mathon, J. Nucl. Mater., 329-333, 333 (2004).
- [2] T. Yoshitake, Y. Abe, N. Akasaka, S. Ohtsuka, S. Ukai, and A. Kimura, J. Nucl. Mater., 329-333, 342 (2004).
- [3] S. Yamashita, N. Akasaka, and S. Ohnuki, J. Nucl. Mater., 329-333, 377 (2004).
- [4] S. Uki, S. Mizuta, M. Fujiwara, T. Okuda, and T. Kobayashi, J. Nucl. Sci. Technol., 39, 778 (2002).
- [5] S. Ukai, and M. Fujiwara, J. Nucl. Mater., 307-311, 749 (2002).
- [6] H.Y. Kim, O.Y. Kwon, J. Jang, and S.H. Hong, Scripta Mater., 54, 1703 (2006).